Dilatancy fabrics in conglomerates in the Awatere fault zone, New Zealand

JOHN V. SMITH

School of Resource Science and Management, Southern Cross University, P.O. Box 157, Lismore 2480 NSW, Australia. E-mail: jsmith@scu.edu.ou

Abstract- Analysis of fabrics of faulted and unfaulted conglomerate within the Awatere fault zone of New Zealand shows that movement on individual faults was accompanied by dilatancy of the clast fabric. The fabric of unfaulted conglomerate is clast-supported, comprising 78% clasts by area. Individual fault zones studied range in width from 4 to 21 cm and have a clay matrix-supported fabric, comprising 33% clasts by area. The abundance of clay within fault zones indicates a highly plastic matrix intruded from the wall rocks into fault zones during localised dilation of the clast fabric. The shear thickening shear-stress-strain-rate relationship typical of dilatant materials suggests that the observed fabrics are more compatible with faults developing slowly as accommodation structures rather than forming rapidly during seismic movements. A rudimentary analysis of the transfer of the minimum lithostatic load through the conglomerate suggests that contact loads between clasts were significantly less than the strength of clasts determined by point load testing. The results provide a mechanism to support a previous interpretation of the fault pattern in terms of dilatant faulting within an oblique divergent tectonic setting. © 1998 Elsevier Science Ltd. All rights reserved

INTRODUCTION

Increase in volume during deformation is known to be an important influence on the mechanics of failure in brittle and granular materials (Jaeger and Cook, 1976). Such dilatancy is manifest in brittle materials as the formation of microcracks and in granular materials as the movement of rigid particles around each other. In both cases, the dilation of the infinitesimal strain field results in directions of conjugate shear failure which have a dihedral angle less than 90° about the principal shortening directions (Smith and Durney, 1992; Johnson, 1995). Scott (1996) demonstrated the close relationship between brittle and granular behaviour by using the formation of dilatant zones in a granular system as a model of earthquake generating fault systems in the crust. Evidence for the role of dilatancy in brittle rocks has been extensively recorded from cataclastic fault fabrics (e.g. Sibson, 1977). In contrast, the role of non-brittle particulate dilatancy in faulting has not been commonly reported, but may be expected in near-surface faulting of gravels or conglomerates.

This study describes evidence of particulate dilatancy where the Neogene–Quaternary Awatere Fault passes through Neogene conglomerate in northeast South Island of New Zealand (Fig. 1). The Awatere fault zone is part of the active strike-slip Marlborough fault system which transfers movement from the thrust/strike-slip Alpine Fault in the southwest to the Hikurangi subduction zone in the northeast (Norris *et al.*, 1990). The Awatere Fault passes through Late Miocene to Early Pliocene conglomerates that are exposed on 260 m high cliffs at White Bluff southeast of Blenheim. Little (1996) recognised a gradient of decreasing strain northward from the main fault and, within the section of conglomerates investigated here, he found an average fault spacing of 19 m and an average displacement of approximately 1 m. The faults are dominantly oblique normal faults which have an average strike of approximately 30° relative to the Awatere Fault. Little (1996) determined that the cumulative fault displacement represented dextral oblique divergence oriented 40–50° relative to the strike of the Awatere Fault. He interpreted the mixture of oblique normal and normal dip-slip faults to indicate that the angle of oblique divergence was close to the critical angle which separates dominantly strike-slip from dominantly dip-slip minor faults. Constant volume strain analysis suggests that the critical angle is controlled by a cross-over of the magnitude of principal incremental strains which occurs at a divergence angle of 19.5° (McCoss, 1986). In contrast, an infinitesimal strain model supported by experimentation (Smith and Durney, 1992) indicates that the critical angle is controlled by a change of sign of the vertical incremental strain which can occur at a divergence angle of approximately 45°. In that model the orientation of faults is strongly influenced by dilatancy during fault initiation. Thus, the dilatancy faulting model (Smith and Durney, 1992) is compatible with both the critical angle of ~45° and the observation of intrusion of matrix material into fault planes in the Awatere fault zone (Little, 1995).

The purpose of this study is to further investigate the evidence of dilatancy preserved in the fault fabrics and to interpret the implications for fault mechanisms and fault orientations. Digital analysis (using NIH Image from the National Institute of Health, U.S.A.)
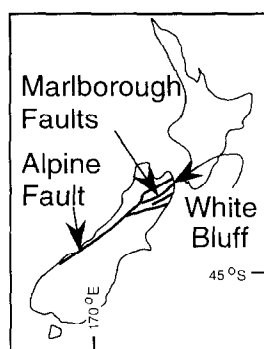
Fig. 1. Location map of the field area at White Bluff, South Island, New Zealand.

of field photographs and samples was used to quantify observations of faulted and unfaulted rock fabrics and point load strength testing was used to supplement interpretations of fault mechanics.

FABRIC STUDY

Numerous faults, including conjugate normal faults (Fig. 2a), cut the conglomerate. This study contrasts the high density of clasts in the fabric of unfaulted rock with a low density of clasts in the fabric of faulted rock (Fig. 2b). Field photographs of faults and adjacent wall rock were enlarged to 17 by 25 cm prints for geometric analysis of the rock fabric.

Unfaulted fabrics

The density of clasts larger than 2 mm, that is larger than sand grade, in unfaulted conglomerate was estimated by image processing of photographs with manual definition of clast boundaries where necessary. Maximum clast sizes within the imaged areas range from 40 to 65 mm (Table 1 & Fig. 3). Wall rock adjacent to fault zones was found to have clast areas ranging from 39 to 64% and numbers of clasts per square metre ranging from 5468 to 10,739 (Table 1); the latter parameter will be used later in discussing the transmission of stress. The role of photographic resolution was investigated by relating the results to the scale of the field photographs used for analysis (Fig. 4). Both average clast area and average number of clasts increase with increasing scale, indicating that both parameters have been underestimated by the technique. One large (30 cm) sample of unfaulted conglomerate was collected so that clast density could be determined on cut faces to allow comparison with the results of field photographs. Cut faces were found to have a clast area of 78% ($n_{clasts} = 308$) and 11,900 clasts per square metre. These values are compatible with the trend of data points in Fig. 4 if an equivalent photographic scale of 1.2 is assigned to them.

Faulted fabrics

The maximum clast size in the imaged areas ranges from 10 to 50 mm (Table 1) and tends to be higher in wider faults (Fig. 3). The presence of unfractured clasts in fault zones (Fig. 2c) and the protrusion of large wall rock clasts into the fault zones (Fig. 2b) indicate that the fabric of fault zones cannot be attributed to cataclastic comminution. Clast density of faulted conglomerate was estimated by the same technique as above and was found to have clast areas ranging from 14 to 29% with an average of 21% (Table 1). The relationship between these values and photograph scale is irregular but shows a positive trend (Fig. 4). No samples of faulted conglomerate were taken to allow a direct comparison between a photographic result and a cut face, so a direct estimate of the underestimation of the photographic method cannot be made. The underestimation of the photographic image analysis technique can be compensated by using the relationship between photographic image analysis of faulted and unfaulted fabrics with respect to the sample of unfaulted rock. According to the photographic method the average ratio of clast area of faulted rocks relative to clast area of unfaulted rocks was 0.42 (Table 1). If this relationship is applied to the clast area of the cut face of the unfaulted specimen (78%) an estimate of 33% area-density of clasts for faulted conglomerate is derived.

Little (1995) illustrated a cut surface of fault rock which was also analysed in this study and found to have an area density of clasts of 22%. This value is just below the low end of the range of values determined from photographic analysis adjusted for underestimation.

POINT LOAD TESTING

In order to constrain interpretation of the mechanics of faulting, specimens of clasts and conglomerate rock were point load tested (Fig. 5). Point load testing approximates the tensile strength of rock by applying a load to an unconfined sample (Franklin et al., 1971; Blyth and de Freitas, 1984, p. 195). The applicability of the results of the point load test is limited by the existence of a confining matrix and the presence of multiple point loads in natural deformation. Confining stresses would increase the strength of clasts such that the point load test provides a lower limit on the strength of clasts. Other tests such as unconfined or triaxial compressive strength of cores from clasts or conglomerate also have limited applicability because they do not account for the effects of the transmission of stress through point contacts.

Clasts failed at point loads from 9 to 34 kN (the upper limit of the manual hydraulic Soilcrete 860-01 Point Load Test Frame). Conversion to point load
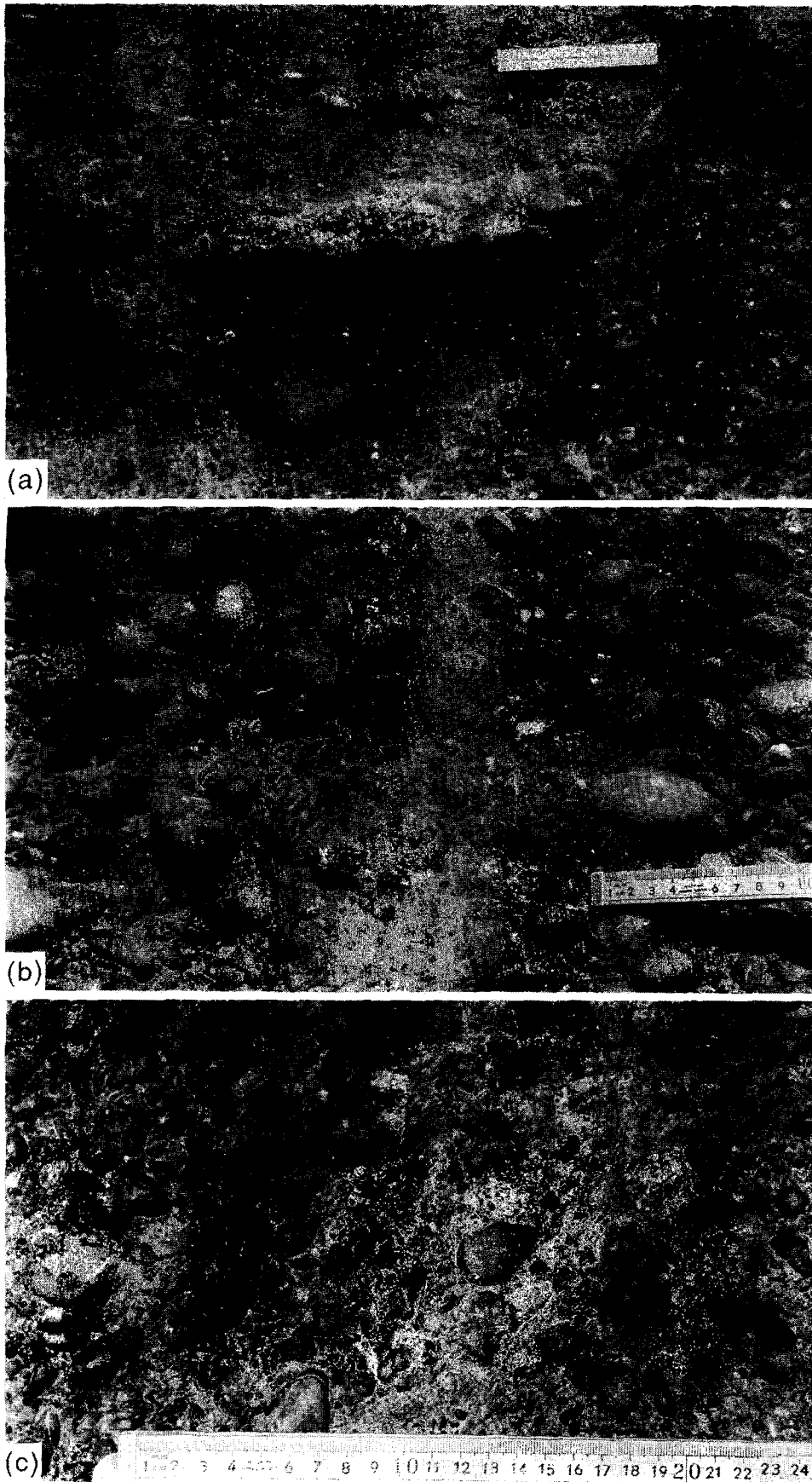
Fig. 2. (a) Conjugate normal faults from the Awatere fault zone (scale bar is 25 cm long). (b) Contrasting density of clasts in unfaulted and faulted (central vertical band) Awatere Conglomerate (Location 2 in Table 1). (c) Unfractured clasts in fault zone (right-hand side) indicating cataclasis is not dominant in the faulting process (Location 1 in Table 1).

Table 1. Fabric data from analysis of field photographs. The impression of a large clast eroded from the exposed surface of the fault zone at location 4 was noted (in brackets) but not used in the fabric analysis

Location	Photo scale	Unfaulted rocks (uf)				Faulted rocks (f)					
		n	size max. (mm)	clast % (area)	clasts/m²	n	size max. (mm)	clast % (area)	fault width (mm)	clast % ratio (f/uf)	adjusted clast %
1	0.98	163	40	49	10103	121	29	24	110	0.49	38
2	0.97	204	62	57	9082	125	22	29	60	0.51	40
3	0.86	283	64	39	6961	177	50	14	210	0.36	28
4	1.0	207	63	64	9395	78	25 (42)	23	50	0.36	28
5	0.74	141	65	60	6737	83	10	19	40	0.32	25
6	0.85	192	60	44	5468	134	21	24	50	0.55	43
7	0.94	185	45	47	10739	142	22	17	150	0.36	28
sample		308		78	11900						

index (division by the square of the sample diameter, see curves in Fig. 5) shows that, except for one clast which failed on a tight joint, the clasts failed at point load indexes above 6 MPa (Fig. 5). Bulk samples of conglomerate failed at point load indexes less than 6 MPa (Fig. 5). These tests were conducted dry and therefore represent an upper bound on the conglomerate strength, which would be lower in the case of a water-saturated clay matrix.

dilatancy of the fabric during flow. The clasts are generally not in contact and dilation of the fabric appears to be beyond the minimum required for granular flow, suggesting that clay continued to migrate into the fault zones as movement occurred.

Little (1996) determined that the Awatere fault zone had undergone dextral divergence directed at approximately 45° to the trend of the fault zone producing the observed pattern of oblique normal faults striking

DISCUSSION

Fault kinematics

For packing of regular spheres, the two-dimensional and three dimensional measures of density are equivalent and vary from 74% for closest packing down to 52% for cubic packing (Graton and Fraser, 1935). Clasts in the unfaulted Awatere Conglomerate are more densely packed than regular spheres due to the influence of poor grain-size sorting (Prince et al., 1995). Clasts in faulted Awatere Conglomerate are less dense than cubic packing of regular spheres, indicating
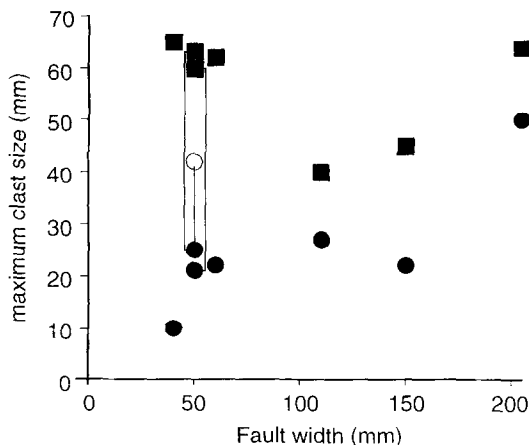

Fig. 3. Maximum grain size of clasts in measured images for unfaulted (squares) and faulted (circles) rocks vs the width of the fault at that location. One of the faults contained the impression of a large clast eroded from the exposure surface (open circle) which was noted but not included in the fabric analysis.

clast area % in faulted rocks
clast area % in unfaulted rocks
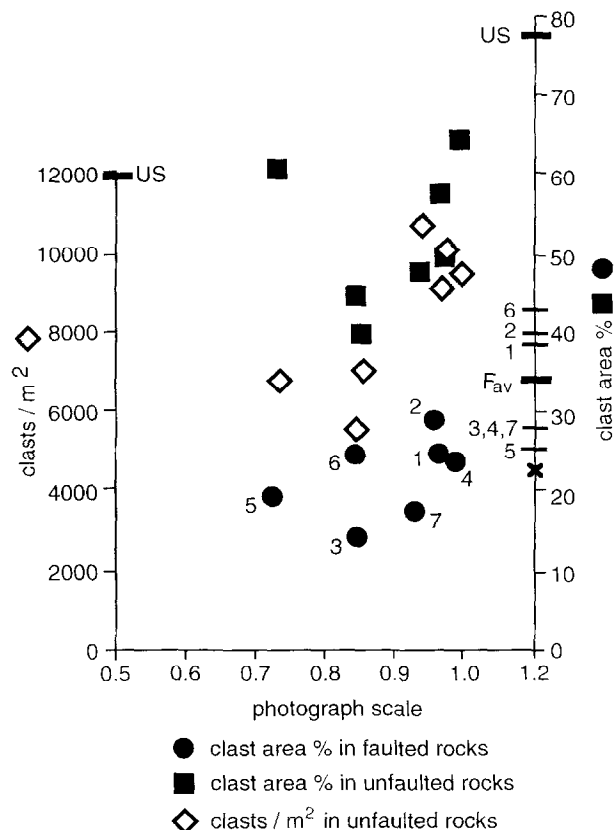clasts / m² in unfaulted rocks

Fig. 4. Measurements of clast area% of unfaulted rocks (squares) and faulted rocks (circles) and clasts/m² in unfaulted rocks (diamonds) related to photograph scale indicating an increase in accuracy with increasing scale. Values determined by analysis of cut faces on a sample of unfaulted rock shown as bars labelled US on the vertical scales. Clast density values adjusted for underestimation of the photographic technique are shown as bars labelled by location number and F_av for the average. Clast area determined for a sample illustrated by Little (1995) is shown as a cross.
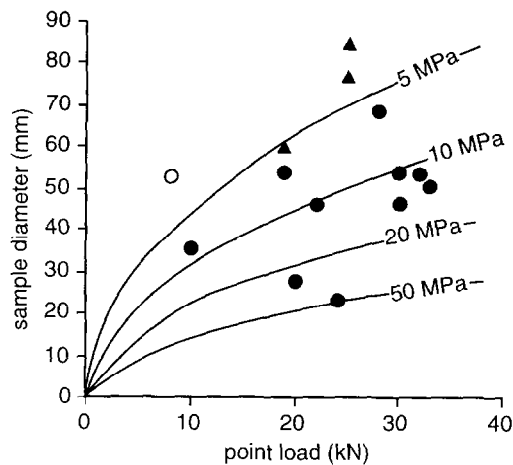
Fig. 5. Results of point load index testing of clasts (circles) and clast-supported conglomerate (triangles). Open circle shows a clast which failed on a stained joint surface. Point load index curves also shown.

~30 clockwise from the Awatere Fault Zone. He recognised this relationship to be compatible with the predictions of the dilatancy faulting model of Smith and Durney (1992). That model was derived from infinitesimal strain analysis of clay models in which the mechanical behaviour was dominated by brittle microcracks. This model is kinematic, rather than mechanical, and is also valid if the dilatancy results from interaction of particles. In the Smith and Durney model, the combination of incremental shortening and volume increase related to dilatancy (Fig. 6a) is responsible for the initiation of faults with a conjugate angle of less than 90 (commonly approximately 60 although the precise angle depends on the specific conditions). When a volume of the rock (Fig. 6b) begins to undergo localised deformation, particle interactions resist simple shear and cause divergent shear (Fig. 6c). Particle interactions will progressively decrease during dilation and the displacement may converge toward
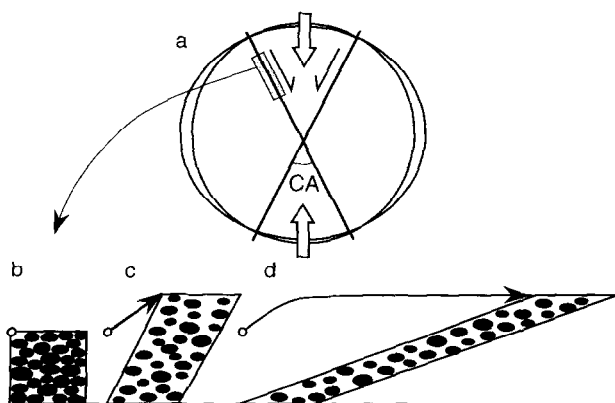

Fig. 6. (a) Illustration of conjugate faults in conditions of incremental shortening (arrows) and volume increase. Because of dilatancy the conjugate angle (CA) is less than 90. The dilatant fault zone (inset) develops from (b) the original close packed fabric into (c) a dilated matrix-supported fabric. (d) Continued faulting of the dilated fault rock tends toward simple shear kinematics.

simple shear (Fig. 6d). A similar kinematic evolution of some brittle faults was described by Smith (1993).

Fault mechanics

In the Awatere fault zone, faults contain both intact and fractured clasts (Fig. 2). Fragmented clasts appear to be isolated in abundant fine matrix material (Little, 1995), suggesting that fractures formed by tensile cracking. Systematic decrease in size of clasts within fault zones, indicative of compressive crushing of clasts, was not observed. The point-to-point stresses generated between clasts during faulting must have been sufficiently low to prevent such extensive crushing of clasts but high enough to crack some clasts or detach them along pre-existing weaknesses. The contrast in strength between the clasts and matrix is sufficiently high for deformation to occur principally by clasts moving around one another.

Particulate dilatancy of the type described here is commonly associated with shear thickening rheological behaviour (Smith, 1997) in which the resistance to flow, or apparent viscosity, of the material increases as the strain rate increases. This rheological consideration supports the proposition that the faults formed by slow aseismic shearing, which Little (1995) considered to be consistent with the shear fabrics observed in fault matrix material.

During deformation of the conglomerate, compressive stress would have been concentrated on clast–clast contacts (Price, 1966) rather than being uniform throughout the rock. The more weak and plastic the matrix, the smaller proportion of the load the matrix would bear. It was estimated above (from the trend of clast densities with respect to image scale) that there are approximately 11,900 clasts/m^2 in the unfaulted conglomerate. The vertical load would be distributed across a horizontal plane through all the point contacts existing between the clasts above and below that plane. For regular spherical clasts each clast would be supported by contact from three clasts whereas for graded non-spherical clasts more point contacts would be expected. A conservative estimate (support by three clasts) of the point contacts per square metre is 35,700. The 50 MPa lithostatic confining pressure interpreted for faulting at White Bluffs (Little, 1995) would produce an average contact point load of 1.4 kN, well below the point load strength of clasts in the conglomerate (Fig. 5).

CONCLUSIONS

Clast-supported conglomerates faulted by movements of the Awatere fault zone have fabrics which record dilatancy of the rock during deformation. The high strength of clasts relative to matrix resulted in clasts moving apart to accommodate shear strain.

Analysis of photographs and samples of unfaulted rocks show 78% clasts by area. In contrast, photographic image analysis of faulted rocks, adjusted for underestimation by the technique, indicates that the clast area decreases to approximately 33% as a consequence of faulting. This observation provides a mechanism to support the dilatancy faulting model of Smith and Durney (1992) in predicting the geometric pattern of minor faulting in the Awatere fault zone. The strain rate dependence of dilatant behaviour in particulate materials supports the interpretation of relatively slow formation of the faults by accommodation of the bulk tectonic strain rather than rapid formation by seismic movements.

REFERENCES

Blyth. F. G. H. and de Freitas. M. H. (1984). *Geology for Engineers*. Edward Arnold, London.

Franklin. J. A., Broch, E. and Walton. G. (1971) Logging the mechanical character of rock. *Transactions of the Institute of Mining and Metallurgy* **80**, 1 9.

Graton. L. C. and Fraser. H. J. (1935) Systematic packing of spheres with particular relation to porosity and permeability. *Journal of Geology* **43**, 785 909.

Jaeger. J. C. and Cook. N. G. W. (1976) *Fundamentals of Rock Mechanics*. Methuen, London.

Johnson, A. M. (1995) Orientations of faults determined by premonitory shear zones. *Tectonophysics* **247**, 161 238.

Little. T. A. (1995) Brittle deformation adjacent to the Awatere strike-slip fault in New Zealand: Faulting patterns, scaling relationships, and displacement partitioning. *Geological Society of America Bulletin* **107**, 1255 1271.

Little. T. A. (1996) Faulting-related displacement gradients and strain adjacent to the Awatere strike-slip fault in New Zealand. *Journal of Structural Geology* **18**, 321 340.

McCoss. A. M. (1986) Simple construction for deformation in transpression/transtension zones. *Journal of Structural Geology* **8**, 715 718.

Norris. R. J., Koons. P. O. and Cooper. A. F. (1990) The obliquely convergent plate boundary in the South Island of New Zealand: implications for ancient collision zones. *Journal of Structural Geology* **12**, 715 726.

Price. N. J. (1966) *Fault and Joint Development in Brittle and Semibrittle Rock*. Pergamon. Oxford.

Prince. C. M., Ehrlich. R. and Anguy. Y. (1995) Analysis of spatial order in sandstones II: grain clusters, packing flaws, and the small-scale structure of sandstones. *Journal of Sedimentary Research A* **65**, 13 28.

Scott. D. R. (1996) Seismicity and stress rotation in a granular model of the brittle crust. *Nature* **381**, 592 595.

Sibson. R. H. (1977) Fault rocks and fault mechanisms. *Journal of the Geological Society of London* **133**, 191 213.

Smith. J. V. (1993) Kinematics of secondary synthetic ("P") faults in wrench systems. *Tectonophysics* **223**, 439 443.

Smith. J. V (1997) Shear thickening dilatancy in crystal-rich flows. *Journal of Volcanology and Geothermal Research* **79**, 1 8.

Smith. J. V. and Durney, D. W. (1992) Experimental formation of brittle structural assemblages in oblique divergence. *Tectonophysics* **216**, 235 253.